A New and Efficient Design of Double Pass Solar Air Heater

S. A. Gandjalikhan Nassab [1 *], M. Omid Panah [2]

[1] Mechanical Engineering Department, School of Engineering, Shahid Bahonar University of Kerman, Kerman, Iran

[2] Department of Mechanical Engineering, Technical and Vocational University (TVU), Tehran, Iran

[*] Corresponding author, Email: Ganj110@uk.ac.ir

Abstract: In the present study, a new and efficient design of a double-pass solar air heater with converged air ducts is proposed and simulated numerically. In the designed solar collector, the inclined position of the absorber plate regarding the glass cover and bottom plate provides converged shapes for the upper and lower air ducts, in which the accelerated flows and extra turbulence generation cause an increased rate of convection heat transfer. This concept is evaluated by numerical solution of the governing equations for air turbulent flow consisting of the conservations of mass, momentum, and energy by the finite element method using the COMSOL Multi-physics. Besides, the conduction equation is solved to compute the temperature distributions inside all solid parts. Numerical findings reveal that the increased velocity of airflow inside the converged duct causes significant convection enhancement, especially in the downstream side of airflow with a thick thermal boundary layer. This behavior leads to a considerable decrease in the absorber temperature due to a higher convection coefficient. The air outlet temperature for the studied test case with the inclined angle of 3^0 is found 3.5 C^0 more than that obtained for the base model and the percentage of efficiency increase is calculated about 10% due to using a converged duct.

Keywords: Double pass SAH; converged duct; turbulent flow, Numerical investigation

1. Introduction

Solar air heaters (SAHs) have vast implications in the industry and agriculture [1, 2]. Considering the low efficiency of the air heaters due to the weak conductivity and small heat

capacity of the working fluid, several investigations have been performed for convection enhancement by different techniques. Suggestions included designing concave and convex airflow channels [3], applying wire-mesh packed beds [4], employing fins and extended surfaces with various geometries [5], proposing various shapes of air ducts [6], as well as utilizing radiating gas, such as carbon dioxide inside a closed-loop consisting the solar collector and an extra heat exchanger [7, 8].

One of the methods for convection augmentation is using a vortex generator to mix flow and break the thermal boundary layer [9]. In the analysis, flow equations were solved by the finite element method using a two-way strongly-coupled Fluid Solid Interaction (FSI) between a thin elastic winglet and transient turbulent natural convection airflow inside a solar chimney. Findings showed a considerable performance development of SAH compared to a clean solar air chimney. About a 9% decrease in the average absorber temperature and a 56% enhancement in the convective airflow rate was seen because of the generated vortices by the applied flapping winglet.

Employing the converged air duct in single-pass SAHs was considered as a useful method for enhancing the thermal performance of solar collectors by Gandjalikhan Nassab [10]. In the investigated plane SAH, the inclined glass cover created a converged form of an air duct having a specific contraction ratio. To this end, the FEM was employed to solve a set of governing flow equations as well as the Laplace equations for solid parts of the collector. The findings indicated that the converged shape of the air duct has a potent potential in designing efficient SAHs, especially under a high converging ratio. Based on the numerical findings, the accelerated airflow causes a decrease in thermal boundary layer thickness, and the existence of extra turbulence leads to the convection enhancement. A numerical study was conducted by Zho et al. [11] to examine the convective heat transfer enhancement and friction loss behavior for turbulent flow in SAHs by using arrays of differently shaped ribs combined with the delta-winglet vortex generators. The numerical finding revealed that applying vortex generators combined with the 60° V-shaped continuous ribs contributes to the best result. The effect of miniature V rib-dimple hybrid structures on the turbulent flow structure was studied numerically by Ran et al. [12] at different rib heights, dimple depths, rib pitches, and rib-to-dimple pitches. It was found that the vortex

flow induced by the V-rib leads to a significant convection enhancement. A similar study about the SAH performance enhancement with differently shaped miniature combined with dimple-shaped roughness has been reported by Arya et al. [13] with numerical and experimental methods. A comprehensive literature review on history, fundamentals, and the latest advancement reported in the field of solar thermal air heating systems was done by Goel et al. [14]. In that study, various designs of solar collectors were presented and discussed. Multi-objective optimization of cylindrical shape roughness parameters in SAHs was done by Azadani and Gharouni [15] and the optimum values of some important parameters such as roughness diameter, height, and longitudinal pitch were examined. The performance enhancement of SAHs with differently shaped miniature combined with the dimple-shaped roughness was studied by Arya et al. [13] and the effects of geometrical factors on efficiency increase were examined. The numerical study by Gandjalikhan Nassab and Sheikhnejad [16] showed that the use of a vortex generator in double-pass SAHs enhances the convection heat transfer via mixing and generating high turbulence region inside the airflow. The heat transfer enhancement in solar air heaters using polygonal-shaped ribs and grooves was studied by Taler et al. [17]. Numerical findings revealed a high Nusselt number of 3.762 at the optimum values of the geometrical factors.

As noted before, a great number of techniques for improving the performance of SAHs has been studied by many investigators. In this regard, the effect of using converged ducts in the single pass SAHs for convection enhancement was examined by the first author [10]. Regarding the existence of two air ducts in double pass SAHs and more rate of heat transfer between the airflow and absorber due to the large surface area, it is expected that this technique leads to a better result and more convection augmentation. Thereby, the authors decided to examine the effect of converged air ducts on the performance of double pass SAHs for the first time by designing a movable absorber plate that can rotate about its central axis. This simple method provides the converged shapes for both upper and lower air ducts in the solar collector (Fig. 1). So, in the present investigation, a plane double-pass SAH is introduced with a nozzle-shaped air ducts and analyzed by numerical solution of the governing equations using the COMSOL Multi-physics. Numerical findings are shown in the forms of temperature, velocity, and pressure contours and also the variations of important parameters with the absorber till angle. Since the applied technique can be employed easily

by designing a movable absorber plate that can rotate about its central axis, it is expected that the present study can facilitate the design of more efficient double-pass SAHs, practically.

2. Theory

Figure 1 illustrates a schematic of the analyzed solar collector. The length of air heater equals to L=1 m, and the airflow thickness in both upper and lower air ducts in the case of zero absorber inclined angle (base model) is denoted by b with the value of 4 cm. The system has the capability of the absorber plate rotation around its central point A in the range of $0 \leq \alpha \leq 5.2^0$. Table 1 presents the values of physical characteristics and geometrical factors of each part in the investigated SAH. The Reynolds number $\rho \bar{V} D_h/\mu$, is equal to 2700, corresponding to the turbulent convection flow. Regarding the numerical simulation, a small part of the solar incident radiation, i.e., $\alpha_g . q_{sun}$ is absorbed by the glass cover, a small part, $\rho_g . q_{sun}$ is reflected, and its major part is absorbed by the absorber plate after transmitting from the glass cover. The heat exchange by surface radiation between the glass cover, absorber, and bottom plate is also considered in the computation of the surface heat fluxes. The glass sheet and insulation layer from their external boundaries are exposed to heat transfer with the surroundings. The rate of energy loss from these boundary surfaces is calculated through the equivalent convection coefficient, h_{eq} including both convection and radiation mechanisms.

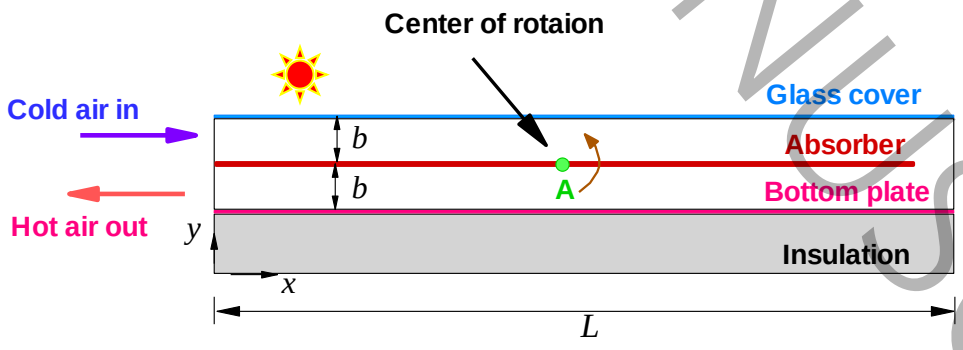

Fig. 1: Double pass SAH with adjustable absorber plate

Since the air temperature inside the SAH varies in a wide range from the high-temperature level of the heated absorber plate to ambient low temperature at the inlet section, the

variations of air density and thermal conductivity with temperature are considered into account. Four various values of the till angle are considered, such that the case of $\alpha = 0$ corresponds to the base model with a constant area duct. The converging ratio, CR=A_{in}/A_{out} for the upper and lower air ducts, which is the same, can be computed as a function of inclination angle, whose values are tabulated in Table. 2.

Table 1: Physical characteristics of solid materials

Element	Length	Thickness	Conductivity	Emissivity	Reflectivity	Transmissivity
Insulation	1 m	40 mm	0.037 W/mK	-	-	0
Bottom plate	1 m	4 mm	400 W/mK	0.98	0.02	0
Glass cover	1 m	4 mm	0.78 W/mK	0.9	0.05	0.9
Absorber	0.96 m	4 mm	400 W/mK	0.98	0.02	0

Table 2: Converging ratio of air ducts at different absorber till angles

α(Degree)	Converging ratio
0	1
1	1.5
2	2.5
3	4.4

2.1 Flow equations and boundary conditions

The theoretical model for investigating the double pass SAH operating in a steady-state is created by the following equation:

$$\nabla.(\rho\vec{U}\varphi) = \nabla.(\Gamma_{\varphi}\nabla\varphi) + S_{\varphi} \qquad (1)$$

In Eq. 1, the dependent variable φ stands for the air velocity, temperature, turbulent kinetic energy, and its dissipation rate. Besides, Γ_{φ} and S_{φ} represent the diffusion coefficient and source term, respectively. More details about Eq. 1 were presented in Ref. [18]. The flow equations are solved using the standard $\kappa - \varepsilon$ model according to the RANS method [19, 20]. In addition, for temperature calculation in solid parts of SAH, the Laplace equation is solved, such that the source term $S_T = \alpha_g q_{sun} / \delta_g$ is considered in the glass cover conduction equation due to the radiation absorption by this element.

In numerical solution, it is assumed that air enters into the double pass SAH with $T_{in=}$ 293 K and developed velocity profile with 0.02 kg/s mass flow rate. Also, the value of kinetic energy of turbulence is set $0.001|V|^2$. In the analyzed test cases, including four different values of the converging ratio, although the surface area of the inlet section varies with the inclination angle, the value of mass flow rate is kept constant and equal to 0.02 kg/2, unless the effect of this parameter is concerned to be examined. At the outlet section, zero pressure is employed for air flow and zero axial gradients in flow direction are considered for the air velocity and temperature. The upper surface of the absorber plate is exposed to a constant heat flux, $q_{sun} \times \tau_g \times \alpha_{abs}$, and the temperature and heat flux continuities are used at the air-solid interfaces. The convection boundary condition is employed on the outer surfaces of the heater adjacent to the surroundings, such that the equivalent coefficient, $h = h_{conv} + h_{rad}$ is computed as [21]:

$$h_{conv} = 5.7 + 3.8V_{wind} \tag{2}$$

$$h_{rad} = \sigma\varepsilon_g \left(\frac{T_g^4 - T_{sky}^4)}{T_g - T_{amb}}\right) \tag{3}$$

In Eq. (3), the sky temperature is evaluated by the following relation [21]:

$$T_{sky} = 0.0522T_{amb}^{1.5} \tag{4}$$

3. Grid study

Due to the existence of an inclined absorber plate in the computational domain, the mapped discretized domain could not be used, thereby the unstructured grids with triangular shapes were created and employed for meshing. In grid independent study, a double pass SAH with a converging ratio of 2.5 was modeled and simulated considering the number of grids ranging from 17232 to 29778 under similar operating conditions. The percentage deviation in the value of maximum temperature that takes place on the absorber plate as a sensitive parameter to the grid size is assessed and reported in Table 3. The relative deviation in the value of this parameter became less than 0.09% from 24815 to 29778 grids. Thereby, based on the results

obtained in the grid study, the third mesh size with 24815 elements was used in further simulation as the optimum grid size. A schematic of the meshing is shown in Fig.2.

Table 3. Results of grid study

No	Number of elements	T_{max} (K)	Percentage of variation
1	17232	311.5	-
2	20679	325.5	4.5
3	24815	328.3	0.86
4	29778	328.6	0.09

Given the application of the wall function approximation for the computation of air velocity at the grid points adjacent to the solid boundaries, the minimum size of grid nodes was selected to satisfy, $y^+ \geq 30$ lying out of the buffer zone in turbulent forced convection flow [20].

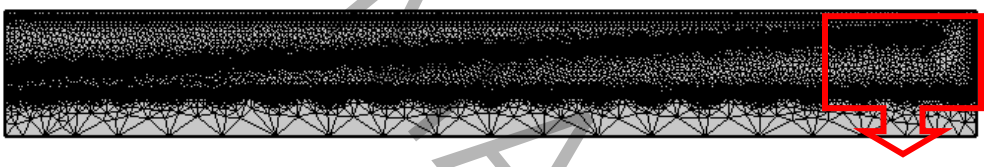

a) The whole of the discretized computational domain

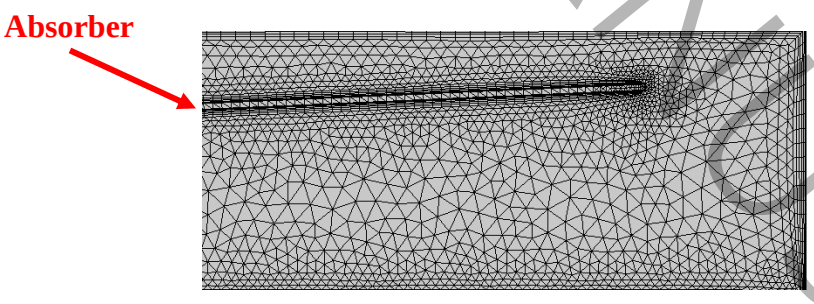

b) Grids inside the air flow domain near the end of absorber plate

Fig. 2: The triangular unstructured grid

For validating the applied numerical model, a comparison of the experimental thermal efficiencies with the predicted ones in the present study has been employed and displayed in Fig. 3 for both single and double-pass SAHs. These solar collectors have been investigated by Chabane et al. [22] and Ramani et al. [23] experimentally. Both experimental and

theoretical findings demonstrate an incremental trend for thermal efficiency as the incoming solar irradiation gets higher values. The positive impact of air mass flow rate on thermal efficiency is also observed in Fig. 3-a. Moreover, the maximum deviation in thermal efficiencies between the numerical and experimental findings are ±4% and ±6% for the studied single and double-pass solar air collectors, respectively. Thereby, a good consistency is observed between the present results and the experimental findings reported in the literature.

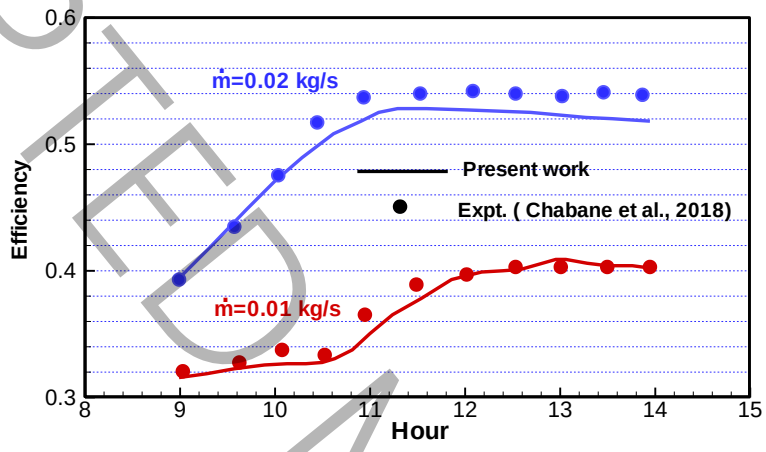

a) Single pass collector

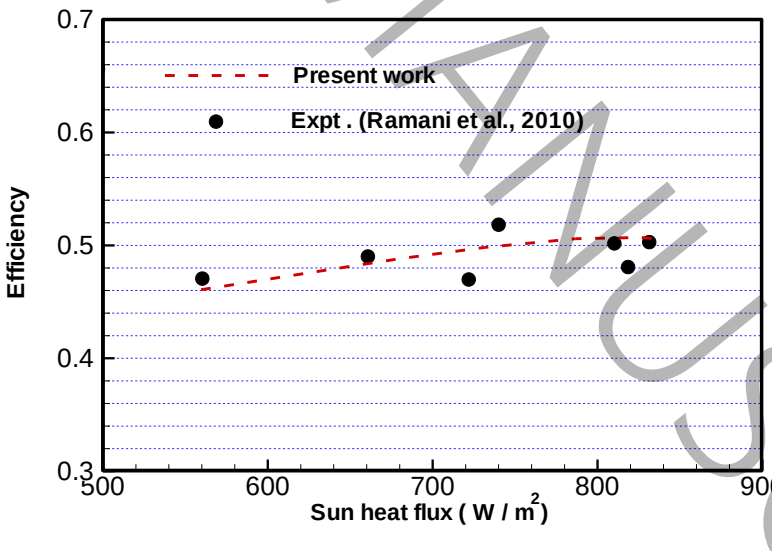

b) Double pass collector

Fig. 3: Variations of thermal efficiency at different operating conditions and comparison with experiment [22, 23]

All of the simulations were carried out using a personal computer with Intel(R) Core (TM) i5-3210M cpu@2.50 GHZ and 4 GB of RAM with a CPU time of 17 minutes.

4. Results and discussion

After validating the grid generation to the model adoption, the COMSOL code was run for different values of the converging ratio, and various results are plotted and discussed in this part. Figure 4 shows the hydrodynamic behavior of the turbulent convection airflow inside the upper and lower ducts of the double pass SAH by plotting the air velocity contours at various absorber plate till angles. After air enters the solar collector with a fully developed velocity, it passes from the air duct with a favorable pressure gradient by a blower. In the case of $\alpha = 0^0$, the convective flow remains at its completely developed velocity profile along a great part of the heater duct, and as the flow returns into the second pass, a recirculated zone takes place because of the separation. Moreover, low-speed bulk fluid is observed at two right corners. The heat transfer rate decreases in all these low-spead zones forming two local high-temperature domains. However, for the cases with the converged shape of the air channels, the airflow presents a positive acceleration due to the mass conservation criterion, and the value of maximum velocity inside the flow domain increases. Such phenomenon is exaggerated at the condition of high values of the absorber till angle, in which the extent of the recirculated domain in the lower duct enlarges and the air velocity gets higher values. The positive acceleration and then the momentum exchange inside the convective flow cause higher rates of convection heat transfer with the heated surface.

$a)\alpha = 0^0$

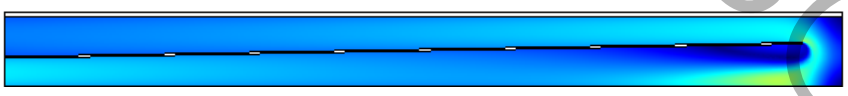

$b)\alpha = 1^0$

$c)\alpha = 2^0$

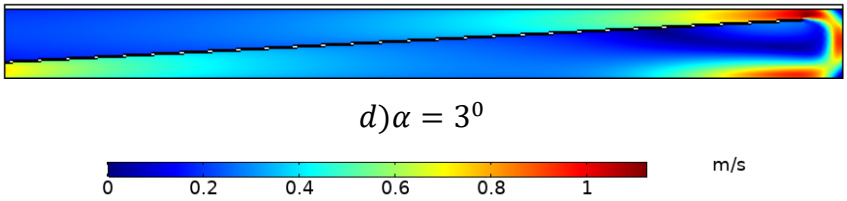

$d)\alpha = 3^0$

Fig.4: Contours of velocity magnitude at different absorber till angles

The temperature contours within the whole domain of SAH are plotted in Fig. 5 at various values of the absorber plate till angle. The contour plots show high-temperature regions near the absorber surface and also adjacent to the bottom plate inside the insulation layer. This behavior is clearly seen in the zoomed figure, which shows the maximum temperature belongs to the absorber plate. It is seen from Fig. 5 that a large value of absorber till angle signifies higher air velocity under which the thermal boundary layer thickness is decreased. Given that the boundary layer growth is an adversary to heat removal, the thinner boundary layer is expected to show higher rates of heat removal. This is clearly observed from the contour plots indicating that the heat transfer process improves significantly at higher absorber inclination angle.

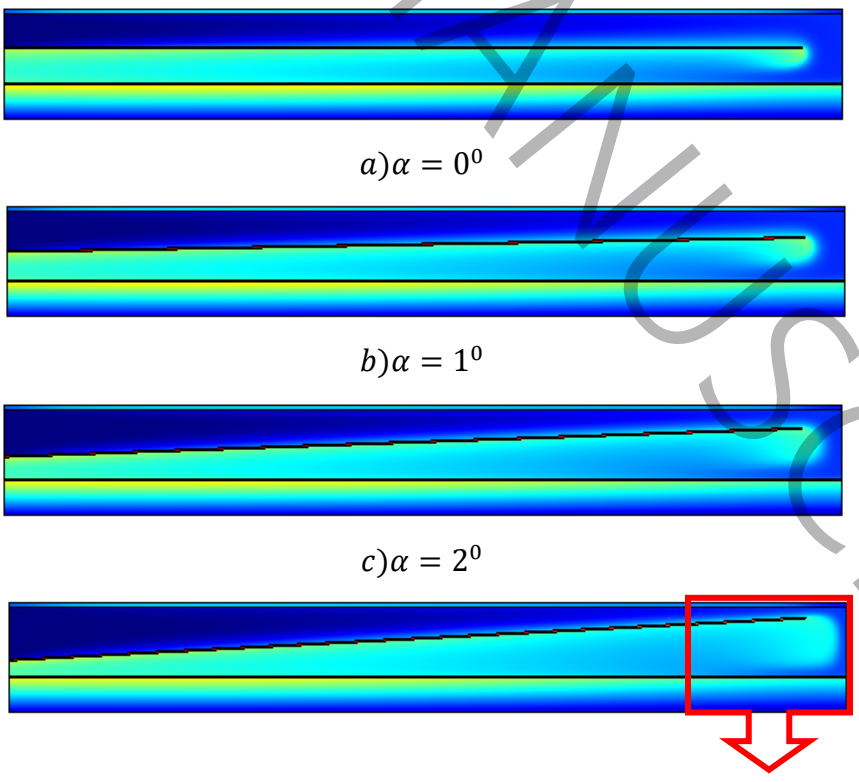

$a)\alpha = 0^0$

$b)\alpha = 1^0$

$c)\alpha = 2^0$

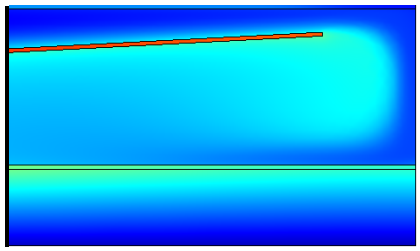

$d)\alpha = 3^0$

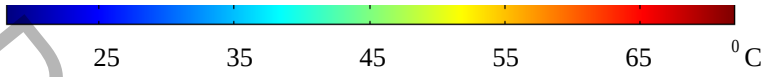

Fig. 5: Temperature contours at different absorber till angle

In Fig.6, the dependency of pressure variation with the converging ratio is investigated by plotting the pressure contours at various till angles. As represented, the air pressure decreases in the base model ($\alpha = 0^0$) is just attributed to the viscous friction, but for SAHs with inclined absorbers, the velocity increase in the converged ducts along the flow direction is the second factor. However, most pressure loss occurs at the upper duct near to the end of absorber plate, where flow turns 180º. A comparison among the pressure fields depicted in Fig. 6 indicates higher pressure drop in the cases with more inclination angle, such that the air pressure inside the first pass becomes much higher than the second pass due to blockage effect and returning the airflow at the end of upper duct.

$a)\alpha = 0^0$

$b)\alpha = 1^0$

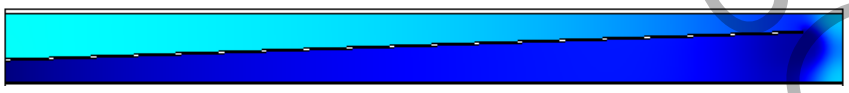

$c)\alpha = 2^0$

$d)\alpha = 3^0$

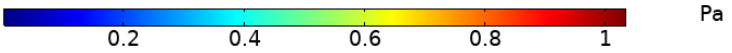

Fig. 7 : Air pressure contours at different absorber till angles

For having a clear image of the thermal behavior of SAH, the temperature variations in the y-direction across the solar collector including the convective air flow and all solid parts at two different absorbers till angles and also at three different axial sections are drawn in Fig. 8. Different trends for temperature variation, especially for the convection airflow in two heater ducts can be seen in this figure. This is due to having different air duct heights by changing the inclination angle. The temperature decreases in the glass cover and absorber plate by increasing in inclination angle are two desired phenomena, which lead to a higher efficiency. If one compares the temperature distributions of the airflow in the second pass at *x=L/4* for the base model and the test case with $\alpha = 3^0$, it can be found that a higher rate of energy conversion in the SAH with an inclined absorber takes place as a result of flow acceleration. As Fig. 8 shows, in all of the three axial sections, the average air temperature in the second pass for the case of inclined absorber is higher than the base model. Besides, the insulation temperature also decreases slightly by increasing in the absorber till angle, and this behavior leads to less heat loss and higher performance.

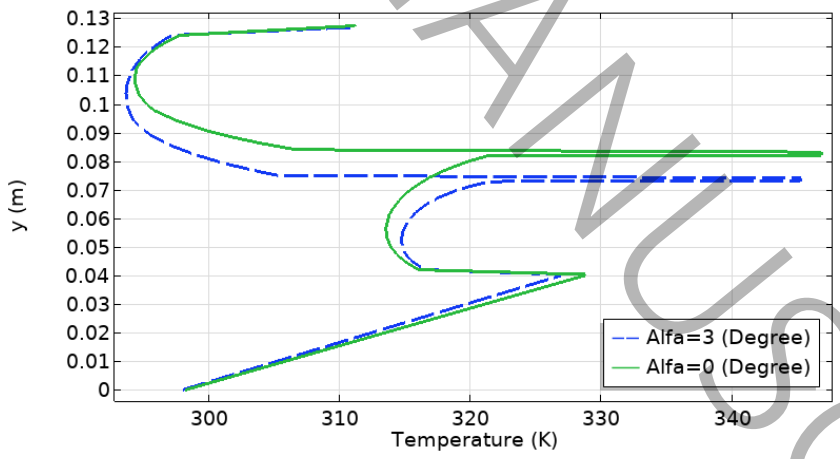

a) X=L/4

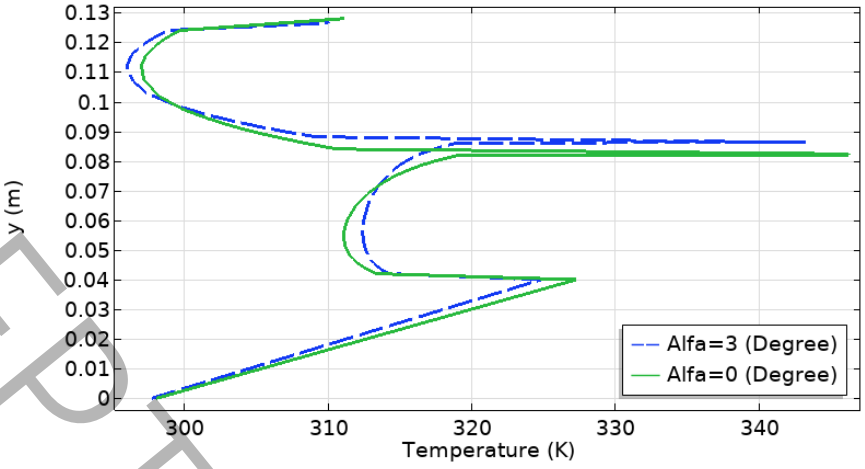

b) X=L/2

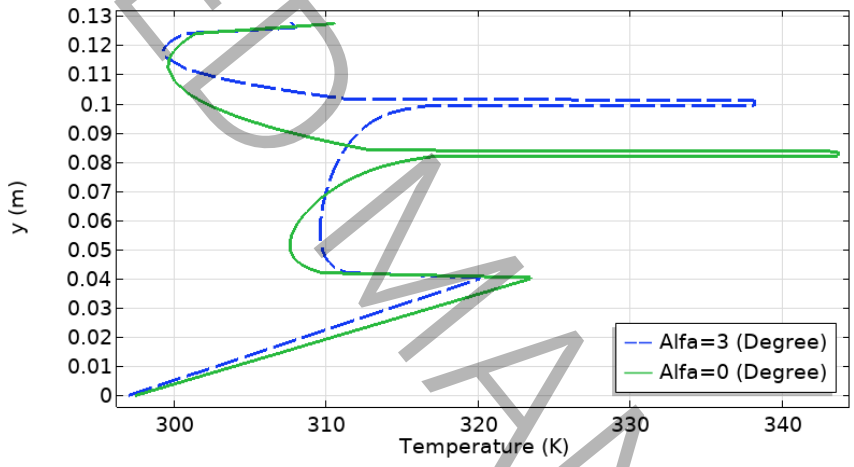

c) X=3L/4

Fig. 8: Temperature variations along the y-direction at two different absorber till angle

Since the SAH efficiency is affected by the outlet air temperature as the main factor, the working gas temperature variation across the outlet section is plotted in Fig. 9 at different values of the inclination angle. It should be recalled that as the area of the inlet section of SAH varies with the absorber till angle, for having the same operating condition, the air mass flow rate is kept constant in all of the test cases. Figure 9 demonstrates higher air temperature at the outlet section as the angle α gets higher values. This behavior is the main reason for proving the positive impact of converging air ducts on the output of a double pass SAH, such that one can compute more than a 17% increase in the value of $(T_{m\,out} - T_{in})$ compared with

the base model by employing the inclined absorber with $\alpha = 3^0$. The variation of air bulk temperature at the outlet section v.s the inclination angle is drwan in Fig. 10 for two different solar heat flux. The increasing trend of the outlet temperature with increasing in the value of converging ratio also reveals the benefit of the proposed technique in enhancing the rate of heat transfer in double-pass SAHs. Besides, as expected, the air outlet temperature gets higher values when the SAH is exposed against higher solar irradiation.

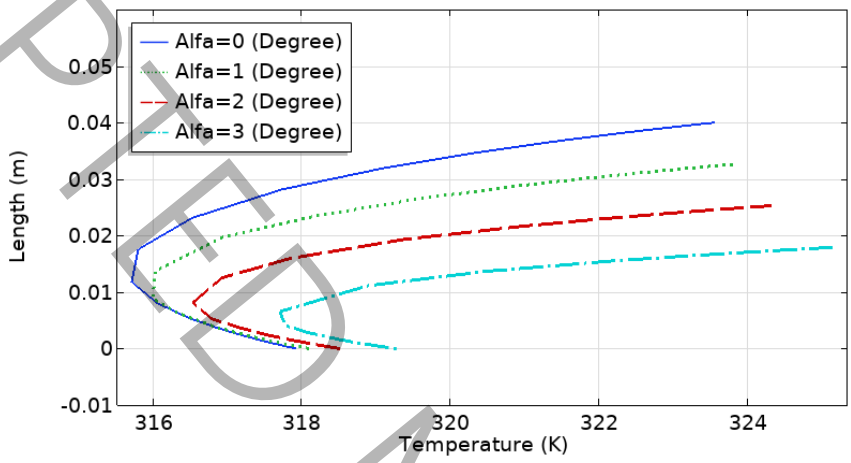

Fig. 9: Air temperature distribution at the outlet section for different absorber till angle

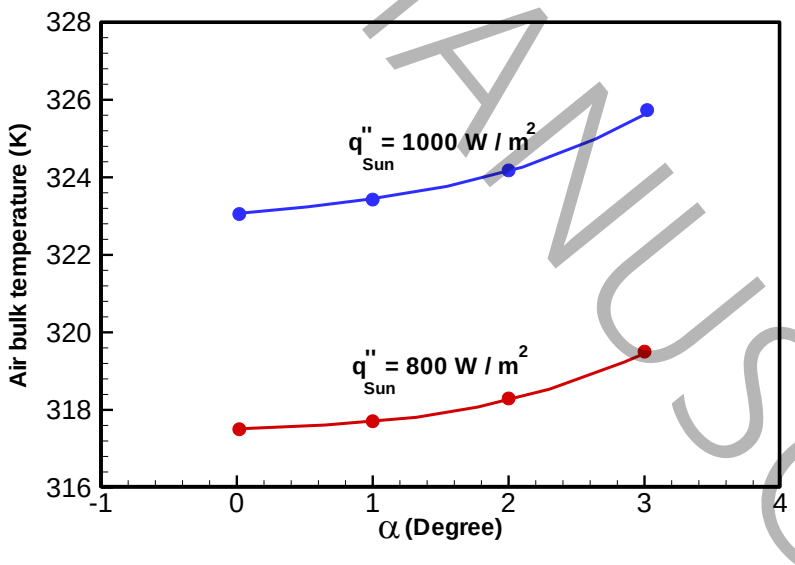

Fig. 10: Variation of air bulk temperature at the outlet section with the angle α at two different incoming Sun heat flum

To demonstrate the positive impact of the flow acceleration on the performance of the solar collector, the temperature distributions along different parts of the heater are illustrated in

Fig. 11 at various values of the angle α. For the base model ($\alpha = 0$), Fig. 11-a shows low temperatures at the two ends of glass cover and the maximum temperature near the middle point with almost uniform distribution in the vicinity of this point. By increasing in the inclination angle, a temperature drop is seen in the glass cover, especially in the second part of this element. This behavior is due to the air velocity increase along the converged air duct and higher rate of convection heat transfer. From Fig 11-a, one can compute about 1.5 ^{0}C decrease in the average value of glass temperature that happens in the case of $\alpha = 3^{0}$. It should be mentioned that the rate of heat loss from the SAH via the glass cover into the ambient decreases with a linear trend by the temperature decrease in this boundary element. In assessing the efficiency of SAH, absorber plate temperature plays an important role. According to Fig. 11-b, the incremental trend of the absorber temperature through the flow direction can be attributed to the increasing thermal boundary layer thickness. Based on Fig. 11-b, the absorber temperature decreases significantly in the cases of using the converged air ducts. At the till angle $\alpha = 3^{0}$, this effect is inhanced, and the absorber temperature decreases at the downstream side of the air duct as a result of a high convection coefficient. Figs. 11-c and d also shows the decreaing trend of the bottom wall and insulation temperatures with increasing in the absorber till angle, but the temperatures of these elements are not much affected by α, compared with the glass cover and absorber.

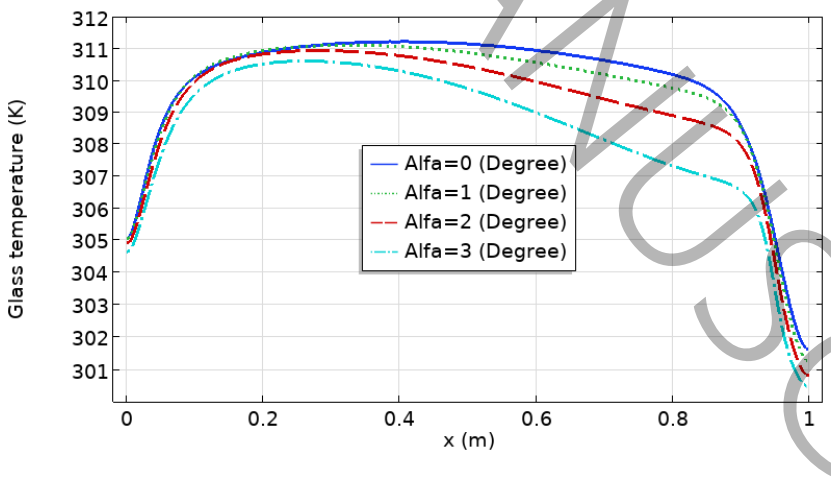

a) Upper surface of glass cover

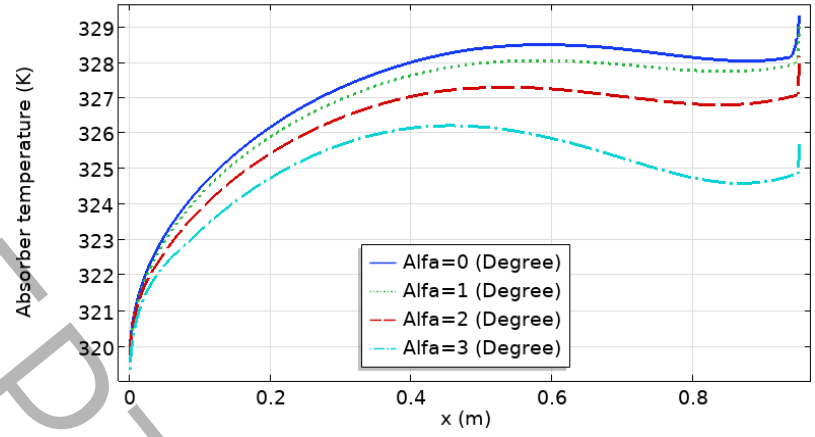

b) Absorber upper surface

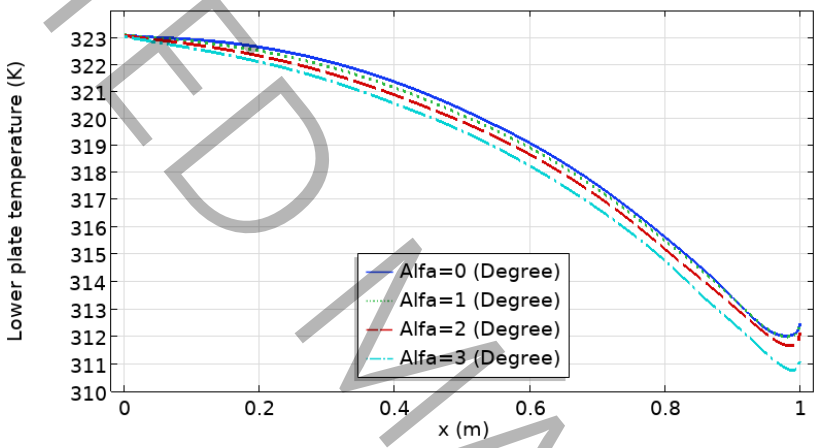

c) Upper sutrface of lower plate

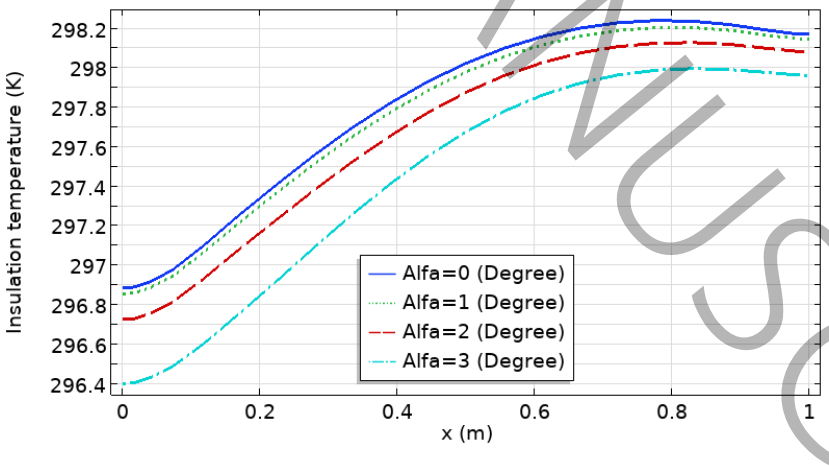

d) Lower surface of insulation

Fig. 11: Temperature distributions along the glass cover, insulation, absorber, and lower plate at different values of the absorber till angles

To demonstrate the positive effect of the inclined angle on the performance of SAH more clearly, the variations of absorber temperature at different axial locations with the inclined angle are drawn in Fig. 12. This figure reveals a lower absorber temperature in the SHA with more inclination, such that in the rangle of $0 \leq \alpha \leq 3^{o}$, the amount of temperature decrease at the axial location *x=2L/3* is about 3.5^{o} C. Considering the phenomenon of surface radiation between the heated absorber plate and the glass cover as a main factor for the heat loss from the solar collector, the decrease in absorber temperature leads to higher thermal efficiency and performance improvement.

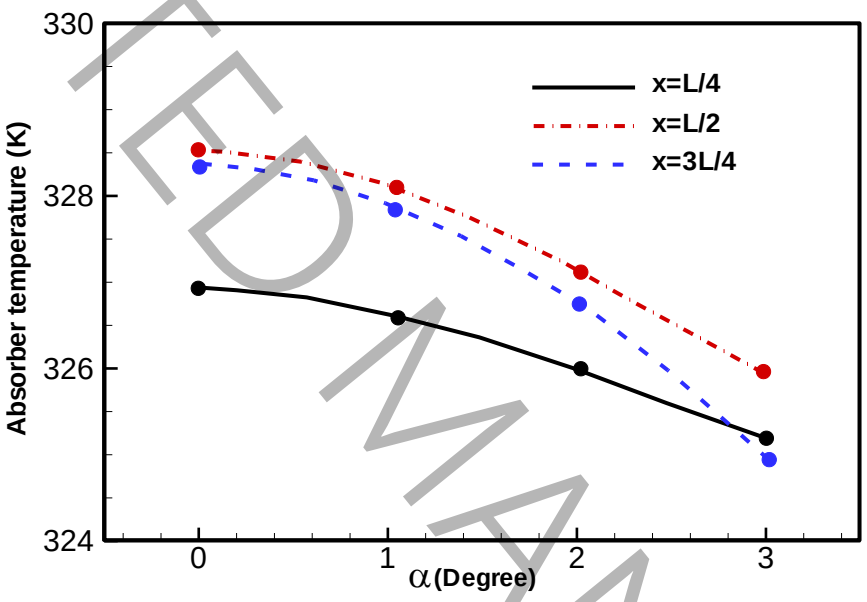

Fig. 12: The variation of absorber temperature at three different locations with the inclination angle

To evaluate the performance of the studied double pass SAH, the thermo-hydraulic efficiency that shows the ability of thermal system to convert solar irradiation into air enthalpy is defined as follows:

$$\eta = \frac{\dot{m} c_p (T_{mout} - T_{in}) - \dot{W}_{fan}}{q''_{sun}.A} \qquad (5)$$

Where, $\dot{W}_{fan} = \frac{\dot{m}\Delta p}{\rho}$. In Fig. 13, the efficiency variation as a function of α at various rates of air mass flow is plotted. This figure shows the efficiency increase by increasing the air mass

flow rate and also reveals the heat transfer augmentation in converged shape air ducts for all operating conditions. The findings also show that the maximum efficiency increase is about 10% at $\alpha = 3^0$ for all air mass flow rates comparing to the base model. Such a significant improvement in the density of double pass SAHs can be obtained easily and leads to design a more efficient double pass solar collector by the proposed technique.

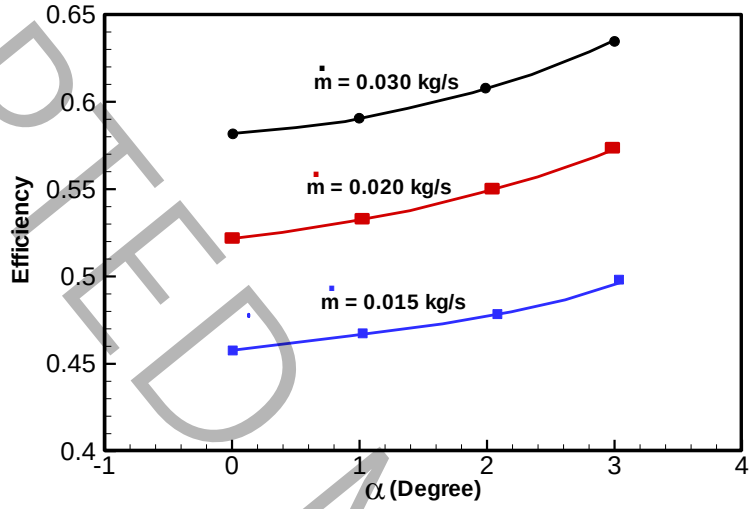

Fig. 13: Variation of thermal efficiency with inclination angle

With regard to the application of the converged channel with a high converging ratio, the increase in pumping power due to the high air pressure drop should be considered. Although a higher rate of convection heat transfer occurs by the use of converged air ducts, this enhancement requires more pumping power. But, the pumping powers' order computed in the studied test cases becomes much less than the energy density of the solar collector (0.02 W compared with 500 W), and can be neglected in the calculation of SAH efficiency.

4. Conclusion

In this research study, the effect of using converged air ducts in double-pass solar collectors for improving thermal performance and providing higher efficiency was examined. To reach this goal, the governing equations, for steady and incompressible 2-D turbulent convection airflow, and the conduction equation for the insulation layer, bottom plate, absorber, and glass cover were solved numerically. The findings revealed that the converged shape of air ducts in double pass SAH proves well its potent potential to design efficient solar collectors. Numerical results showed 10% increase in thermo-hydraulic efficiency of the studied cases

with the converging ratio of *CR*=4.40 compared to the base model. Furthermore, the absorber temperature falls about 3 K, such that this behavior leads to lower rates of heat transfer irreversibility and heat loss from the solar collectors. The glass cover and insulation temperatures are also affected by using converged air ducts, such that the glass temperature is much affected and about 2.8 K decrease in the average temperature of this element was seen for the test case with $\alpha = 3^0$ compared with the base model. So, this theoretical study tried to motivate scholars to mitigate the employment of greenhouse gas and human footprints using high-performance double-pass SAHs.

Funding

This study was not supported or funded by any organizations.

Conflict of interest

Authors declare no conflict of interests regarding the present study.

Nomenclature

A	Area ($\mathbf{m^2}$)	$\boldsymbol{\alpha_g}$	Glass absorptivity
b	Air duct's Height (m)	δ	Thickness (m)
CR	Converging ratio	ϵ	Turbulent dissipation (m^2/s^3)
$\boldsymbol{C_p}$	Specific heat (kJ/kg K)	$\mathcal{E}$	Surface emissivity
$\boldsymbol{D_h}$	Hydraulic diameter (m)	$\boldsymbol{\kappa}$	Turbulence kinetic energy (m^2/s^2)
h	Convection coefficient ($Wm^{-1}K^{-1}$)	ρ	Fluid density (kg/m^3)
k	Thermal conductivity ($Wm^{-1}K^{-1}$)	ρ_g	Glass reflectivity
L	Length of heater (mm)	τ_g	Glass transmissivity
$\dot{\boldsymbol{m}}$	Mass flow rate (kg/s)	φ	Dependent variable
p	Pressure (Pa)	**Subscript**	
q	Heat flux (W/m^2)	abs	Absorber
Re	Reynolds number ($\rho\overline{V_{in}}D_h/\mu$)	amb	Ambient
T	Temperature (K)	eq	Equivalent
$\vec{\boldsymbol{U}}$	Velocity vector (m/s)	in	Inlet
(x, y)	Coordinates (m)	ins	Insulation
Greek symbols		m	Mean
$\boldsymbol{\alpha}$	Absorber till angle (Degree)	out	Outlet

References

[1] M. Aramesh, M. Ghalebani, A. Kasaeian, H. Zamani, G. Lorenzini, O. Mahian, S. Wongwises, A review of recent advances in solar cooking technology, Renewable Energy, 140 (2019) 419-435.
[2] S.A. Kalogirou, Solar thermal collectors and applications, Progress in energy and combustion science, 30(3) (2004) 231-295.
[3] A.P. Singh, O. Singh, Thermo-hydraulic performance enhancement of convex-concave natural convection solar air heaters, Solar Energy, 183 (2019) 146-161.
[4] S. Singh, Experimental and numerical investigations of a single and double pass porous serpentine wavy wiremesh packed bed solar air heater, Renewable Energy, 145 (2020) 1361-1387.
[5] M. Nemś, J. Kasperski, Experimental investigation of concentrated solar air-heater with internal multiple-fin array, Renewable Energy, 97 (2016) 722-730.
[6] A. Beniaiche, A. Ghenaiet, B. Facchini, Experimental and numerical investigations of internal heat transfer in an innovative trailing edge blade cooling system: stationary and rotation effects, part 1—experimental results, Heat and Mass Transfer, 53 (2017) 475-490.
[7] M. Foruzan Nia, S.A. Gandjalikhan Nassab, A.B. Ansari, Numerical simulation of flow and thermal behavior of radiating gas flow in plane solar heaters, Journal of Thermal Science and Engineering Applications, 12(3) (2020) 031008.
[8] A. Dehghani Rayeni, S. Gandjalikhan Nassab, Effects of gas radiation on thermal performances of single and double flow plane solar heaters, International Journal of Engineering, 33(6) (2020) 1156-1166.
[9] Y. Sheikhnejad, S.A.G. Nassab, Enhancement of solar chimney performance by passive vortex generator, Renewable Energy, 169 (2021) 437-450.
[10] S. Gandjalikhan Nassab, Efficient design of converged ducts in solar air heaters for higher performance, Heat and Mass Transfer, 59(3) (2023) 363-375.
[11] Z. Zhao, L. Luo, D. Qiu, Z. Wang, B. Sundén, On the solar air heater thermal enhancement and flow topology using differently shaped ribs combined with delta-winglet vortex generators, Energy, 224 (2021) 119944.
[12] S. Ran, P. Zhang, Y. Rao, Numerical study of heat transfer and flow structure over channel surfaces featuring miniature V rib-dimples with various configurations, International Journal of Thermal Sciences, 172 (2022) 107342.
[13] N. Arya, V. Goel, B. Sunden, Solar air heater performance enhancement with differently shaped miniature combined with dimple shaped roughness: CFD and experimental analysis, Solar Energy, 250 (2023) 33-50.
[14] V. Goel, V. Hans, S. Singh, R. Kumar, S.K. Pathak, M. Singla, S. Bhattacharyya, E. Almatrafi, R. Gill, R. Saini, A comprehensive study on the progressive development and applications of solar air heaters, Solar Energy, 229 (2021) 112-147.
[15] L.N. Azadani, N. Gharouni, Multi objective optimization of cylindrical shape roughness parameters in a solar air heater, Renewable Energy, 179 (2021) 1156-1168.
[16] S. Gandjalikhan Nassab, Y. Sheikhnejad, Novel design of natural double-pass solar air heater for higher thermal performance using vortex generator, Scientia Iranica, 29(3) (2022) 1185-1196.
[17] B.V. Kumar, C.P. Selvan, P.R. Kanna, D. Taler, M. Szymkiewicz, J. Taler, Numerical investigation of heat transfer enhancement in solar air heaters using polygonal-shaped ribs and grooves, Frontiers in Energy Research, 11 (2023) 1279225.
[18] L. Tang, W. Chu, N. Ahmed, M. Zeng, A new configuration of winglet longitudinal vortex generator to enhance heat transfer in a rectangular channel, Applied Thermal Engineering, 104 (2016) 74-84.
[19] A.P. Singh, A. Kumar, O. Singh, Designs for high flow natural convection solar air heaters, Solar Energy, 193 (2019) 724-737.
[20] M. Tabatabaian, CFD Module: Turbulent Flow Modeling, Mercury Learning and Information, 2015.

[21] S. Singh, Performance evaluation of a novel solar air heater with arched absorber plate, Renewable Energy, 114 (2017) 879-886.
[22] F. Chabane, N. Moummi, A. Brima, Experimental study of thermal efficiency of a solar air heater with an irregularity element on absorber plate, International Journal of Heat and Technology, 36(3) (2018) 855-860.
[23] B. Ramani, A. Gupta, R. Kumar, Performance of a double pass solar air collector, Solar energy, 84(11) (2010) 1929-1937.